NASA / TM—1999-209388

Inspection of Space Station Cold Plate Using Visual and Automated Holographic Techniques

Arthur J. Decker, Matthew E. Melis, and Kenneth E. Weiland
Glenn Research Center, Cleveland, Ohio

August 1999

The NASA STI Program Office . . . in Profile

Since its founding, NASA has been dedicated to the advancement of aeronautics and space science. The NASA Scientific and Technical Information (STI) Program Office plays a key part in helping NASA maintain this important role.

The NASA STI Program Office is operated by Langley Research Center, the Lead Center for NASA's scientific and technical information. The NASA STI Program Office provides access to the NASA STI Database, the largest collection of aeronautical and space science STI in the world. The Program Office is also NASA's institutional mechanism for disseminating the results of its research and development activities. These results are published by NASA in the NASA STI Report Series, which includes the following report types:

- TECHNICAL PUBLICATION. Reports of completed research or a major significant phase of research that present the results of NASA programs and include extensive data or theoretical analysis. Includes compilations of significant scientific and technical data and information deemed to be of continuing reference value. NASA's counterpart of peer-reviewed formal professional papers but has less stringent limitations on manuscript length and extent of graphic presentations.

- TECHNICAL MEMORANDUM. Scientific and technical findings that are preliminary or of specialized interest, e.g., quick release reports, working papers, and bibliographies that contain minimal annotation. Does not contain extensive analysis.

- CONTRACTOR REPORT. Scientific and technical findings by NASA-sponsored contractors and grantees.

- CONFERENCE PUBLICATION. Collected papers from scientific and technical conferences, symposia, seminars, or other meetings sponsored or cosponsored by NASA.

- SPECIAL PUBLICATION. Scientific, technical, or historical information from NASA programs, projects, and missions, often concerned with subjects having substantial public interest.

- TECHNICAL TRANSLATION. English-language translations of foreign scientific and technical material pertinent to NASA's mission.

Specialized services that complement the STI Program Office's diverse offerings include creating custom thesauri, building customized data bases, organizing and publishing research results . . . even providing videos.

For more information about the NASA STI Program Office, see the following:

- Access the NASA STI Program Home Page at ***http://www.sti.nasa.gov***

- E-mail your question via the Internet to help@sti.nasa.gov

- Fax your question to the NASA Access Help Desk at (301) 621-0134

- Telephone the NASA Access Help Desk at (301) 621-0390

- Write to:
  NASA Access Help Desk
  NASA Center for AeroSpace Information
  7121 Standard Drive
  Hanover, MD 21076

NASA / TM—1999-209388

Inspection of Space Station Cold Plate Using Visual and Automated Holographic Techniques

Arthur J. Decker, Matthew E. Melis, and Kenneth E. Weiland
Glenn Research Center, Cleveland, Ohio

National Aeronautics and
Space Administration

Glenn Research Center

August 1999

Available from

NASA Center for Aerospace Information
7121 Standard Drive
Hanover, MD 21076
Price Code: A03

National Technical Information Service
5285 Port Royal Road
Springfield, VA 22100
Price Code: A03

INSPECTION OF SPACE STATION COLD PLATE USING VISUAL AND AUTOMATED HOLOGRAPHIC TECHNIQUES

Arthur J. Decker
Matthew E. Melis
Kenneth E. Weiland

National Aeronautics and Space Administration
Glenn Research Center
Cleveland, Ohio 344135

SUMMARY

Real-time holography has been used to confirm the presence of non-uniformity in the construction of an International Space Station cold plate. Ultrasonic C-scans have previously shown suspected areas of cooling fin disbonds. But both neural-net processed and visual holography did not evidence any progressive permanent changes resulting from 3000 pressurization and relaxation cycles of a Dash 8 cold plate.

Neural-net and visual inspections were performed of characteristic patterns generated from electronic time-average holograms of the vibrating cold plate. Normal modes of vibration were excited at very low amplitudes for this purpose. The neural nets were trained to flag very small changes in the mode shapes as encoded in the characteristic patterns. Both the whole cold plate and a zoomed region were inspected. The inspections were conducted before, after, and during pressurization and relaxation cycles of the cold plate. A water-filled cold plate was pressurized to 120 psig (827 kPa) and relaxed for each cycle. Each cycle required 5 seconds. Both the artificial neural networks and the inspectors were unable to detect changes in the mode shapes of the relaxed cold plate.

The cold plate was also inspected visually using real-time holography and double-exposure holography. Regions of non-uniformity correlating with the C-scans were apparent, but the interference patterns did not change after 3000 pressurization and relaxation cycles.

These tests constituted the first practical application of a neural-net inspection technique developed originally with support from the Director's Discretionary Fund at the Glenn Research Center at Lewis Field.

INTRODUCTION

Some old and new holographic techniques have been used at Glenn Research Center at Lewis Field (GRC) to inspect a cold plate for cooling fin bond integrity. Several types of cold plates are to be used to cool electronic instruments in the Space Station. This study is limited to Dash 8 series plates. Earlier ultrasonic C-scans showed non-uniformities suspected to be disbonds between the cooling fins and the cold-plate face sheets in several cold plates. Various tests, including the holographic inspections described in this paper, were used to check the quality and integrity of the cold plate and to observe, if any, progressive damage occurring during the pressure cycle tests.

The holographic inspections are particularly interesting; since they include the first practical application of a new processing method that uses artificial neural networks. This method[1-4] was developed originally with support from the GRC Director's Discretionary Fund. The neural nets can detect very small changes in interference patterns generated from holograms of a structure. These small changes in the interference patterns, in turn, reflect structural changes. The structural changes might be caused by cracking or by de-bonding as in the case of the cold plates.

Both an ancient and a relatively modern form of holographic interferometry were used to inspect the cold plate. The ancient technique, called real-time holography, used silver-halide emulsions to record the holograms. This technique confirmed the presence of the non-uniform patterns detected by the C-scans. The relatively modern technique, known variously as electronic holography, television holography, or electronic speckle pattern interferometry (ESPI), was used to record the mode shapes of a vibrating cold plate at several different resonant frequencies. The cold plate was excited to vibrate with either a siren or a piezoelectric shaker. The mode shapes, displayed in the form of so-called characteristic patterns, were inspected visually for changes resulting from repeated pressurization and relaxation of the cooling passages. The mode shapes were also inspected continuously and automatically at 30 frames per second by artificial neural networks. The neural networks did detect changes in the characteristic patterns upon pressurization of the cold plate to 120 psig (827 kPa). But neither the human inspectors nor the neural networks detected significant changes in the characteristic patterns of the relaxed cold plate, even after 3000 pressurization and relaxation cycles and in-spite of the non-uniform structure shown by the C-scans and by real-time holography.

This paper discusses the test setup used to conduct these tests and presents and discusses the results of the tests.

TEST SETUP

Tests were conducted at GRC in a laboratory that has been used for holographic testing for the past 23 years. The cold plate was bolted to a frame, and the combination was bolted to a large vibration-isolation table. Front and rear views of the cold-plate and frame combination are shown in Fig. 1.

Knowledge of the detailed construction[5] of the cold plate is irrelevant to execution of the holographic tests; since tests are conducted essentially the same way for any kind of object. The following properties and features define the cold plate adequately for this test. The plate, including fittings, is 37.2 in. (94.4 cm.) wide by 10.2 in. (26.0 cm.) high with through holes on 2 in. (5.1 cm.) centers horizontally and 2.75 in. (7.0 cm.) centers vertically. There are holes on 4 in. (10 cm.) centers along the top and bottom edges. The bottom edge is bolted to the frame and the top edge is screwed to the frame through the holes along the top and bottom edges.

The bolts are set to fixed torque. Best practice requires that all fasteners be set to fixed torque in order to maintain a consistent setup should the panel need to be removed and replaced. The neural networks are very sensitive and have detected small changes in

mode shape resulting from a change in bolt torque.[2] Inconsistent mounting would most likely lead to the need for the neural nets to be retrained to establish a new base line. The cold plate is painted flat white to create a diffusely reflecting surface; since both holographic techniques used for these tests are versions of diffuse-illumination holographic interferometry. The cold plate has inlet and outlet fittings for the cooling water. For the tests, one fitting is capped, the cold plate is filled with water, and the other fitting is connected through an electrically operated, regulating valve to a 120 psig (827 kPa) air supply. A pressurization and relaxation cycle takes 5 seconds leading to a 0.2 Hz cycle rate.

The details of neural-net and holographic technology are very interesting, but far outside the scope of this paper. The book by Charles Vest[6] provides a good reference on the application of holography to structural and flow diagnostics. The neural-net procedures and performance are discussed in the first four references. There are references on the history of diffuse-illumination and electronic holographic interferometry at GRC.[7-10] The electronic holography technique used for the cold-plate tests is discussed by Stetson and Brohinsky.[11]

The bare essentials of holography necessary to understand the cold plate tests are presented below. Figure 2 shows one setup used for holography.

An optical hologram of a structure is always a recording of the interference pattern between the light reflected from the structure and a reference beam. The two beams of light originate from the same laser. An argon-ion laser was used for the cold-plate tests. A hologram was recorded on a high-resolution silver-halide emulsion for real-time holography and on a CCD array for electronic holography. Regardless, the mathematical representation of a hologram contains four terms, and only one or two of those terms are useful. The useful term or terms are extracted in completely different ways for the silver-halide-emulsion and electronic implementations.

The silver-halide-emulsion technique extracts the useful term optically in the form of a phase-accurate reconstruction of the original object light wave. Hence, holography has been thought of historically as a way to reconstruct three-dimensional views of objects. In the real-time technique used for these tests, the reconstructed object wave is interfered with light reflected from the actual object. The real-time interference pattern encodes point-by-point the real-time optical path differences between the original object (frozen in the hologram) and the real-time object. The real-time cold plate, of course, is being deformed by pressurization during these tests.

Holograms are formed essentially the same way for electronic holography. But the silver-halide emulsion is replaced by an optical front end called the speckle interferometer, by a CCD camera, and by a computer workstation with frame grabber. The electronic holograms are actually recorded from lens-formed images of the cold plate rather than the cold plate directly; the holograms are called focused-image holograms. The holograms are recorded at a rate of 30 holograms per second, and the reference beam is phase shifted by π for every other hologram. Time-adjacent holograms are subtracted to extract the two useful terms. Processing, of course, occurs in the computer. The cold plate is excited to vibrate at a resonance while recording an electronic hologram. Holograms, recorded in this manner, are sometimes called time-average holograms; since the exposure is the

average of one or more vibration cycles. Averaging occurs in each television field of the CCD camera for 1/60 second. The resolution of both the hologram and the resulting images is much lower for the electronic holograms than the silver-halide holograms. Holograms and images occupy 486 by 640 square pixels.

Although the holographic techniques seem complex, the outputs of the tests can be stated succinctly in mathematical form. Our implementation of electronic time-average holography produces a pattern proportional to the square of

$$(\text{Speckle Pattern}) * J_0(2\pi K \bullet \delta)$$

where J_0 is the zero-order Bessel function of the first kind; δ is the amplitude of the vibration displacement vector expressed in multiples of the wavelength of the laser light at atmospheric pressure (514.5 nm); and K is called the sensitivity vector. The maximum value of the argument of the Bessel function is $4\pi|\delta|$. For a flat object like the cold plate located about 7 ft. (2.13 m) from the optical front end, K and δ point nearly in the same direction over the entire cold plate. Hence, the pattern can be thought of roughly as a non-linear map of the magnitude $|\delta|$ of the displacement amplitude vector. The multiplier (Speckle Pattern) is responsible for the grainy appearance of the resulting patterns. A discussion of the origin and nature of speckle statistics is outside the scope of this paper. The overall pattern is sometimes called a characteristic pattern for mathematical reasons.[6]

Figure 3 shows a sample Bessel fringe pattern for a vibrating fan blade in the unlikely case that the reader has never seen such a pattern. The bright areas correspond to zeros of the Bessel function and represent nodes of vibration. The brightness of the pattern is observed to decrease as the amplitude of vibration increases and the maximum values of the oscillating Bessel function decrease in magnitude. The grainy appearance is caused by the speckle effect.

Both real-time and double-exposure silver-halide-emulsion holography produce a pattern proportional to

$$I_1 + I_2 \cos(2\pi K \bullet \delta)$$

where K again is the sensitivity vector; δ is the real-time displacement of a point on the cold plate; and I_1 and I_2 depend on the ratio of the hologram-reconstructed and the real-time beams. The speckle effect is also encoded in I_1 and I_2. In general, particularly for real-time holography, this pattern tends to have low contrast, residual fringes and other extraneous fringes for many reasons: emulsion shrinkage, hologram positioning errors, speckle pattern de-correlation, laser-beam shifts, and air currents. Note that the fringes are cosine fringes. The fringe contrast is constant as $|\delta|$ increases; hence there are no visual hints about the varying magnitude of $|\delta|$ as provided by the Bessel function.

There is enough information to perform a classical holographic test at this point using the following procedure. First, electronic holography is used to identify the resonances of the vibrating cold plate as follows. The characteristic patterns are displayed on the computer monitor at 30 frames per second. The drive frequency of the piezo-electric shaker is tuned until the characteristic pattern of a resonance begins to appear. The frequency is carefully adjusted to achieve the maximum response. The drive amplitude is

adjusted to produce a pattern based on the operator's experience. A laser interferometer can be used to measure the vibration amplitude at a point so as to allow the mode amplitudes to be reproduced exactly at a later time. The modes can be recorded in a movie or a still. The process is repeated for as many modes as desired.

Second, the cold plate is pressure cycled, and electronic holography can be used to monitor a vibration mode during pressure cycling. The mode identification and recording process is then repeated after the required number of pressure cycles. The whole process can be repeated as many times as desired. Real-time holography can be used to monitor the real-time fringe pattern during steady pressurization. For silver-halide holography, the real-time pattern can be recorded with a CCD camera.

A classical test in the past required that the characteristic patterns be evaluated visually for changes caused by the cycling process. A visual inspection is tedious and not necessarily accurate. The characteristic patterns are complex, particularly at higher frequencies, and may not change very much unless there is a drastic structural failure. Fortunately, artificial neural networks allow the classical holographic inspection process to be automated with increased sensitivity.

Again, only the more essential elements of artificial-neural-net technology are discussed. Consult reference 4 for a more detailed discussion. The simplest implementation of the neural-net technique was used for the cold-plate tests. So-called feedforward neural nets were trained to flag changes in a characteristic pattern. A neural net was essentially trained to produce two outputs; call them same pattern and changed pattern for convenience.

The neural net was trained to respond in this way to input characteristic patterns. One constraint is that the neural net technology can handle only a few thousand pixels. Hence, large pixels, sometimes called rebinned pixels, must be generated. Figure 4 shows the large-pixel coverage for the region of the entire plate between the water inlet and outlet fittings. Figure 5 shows the large-pixel coverage in a zoomed region between four through-holes. A few thousand pixels fortuitously happen to be the number of finite elements used in a typical finite element model of vibration modes. The possible role of finite-element modeling in neural-net inspections of characteristic patterns is discussed in the references.[1-4]

A neural net must meet four requirements to be successful. First, the net must not be fooled by variations in the constantly changing speckle pattern. Our research[1] has shown that a neural net will learn to ignore the laser speckle effect, if the net is trained with uncorrelated speckle sample functions equal in number to 10 percent of the number of input pixels. The training-set software is designed to record arbitrary numbers of uncorrelated speckle sample functions.

Second, the neural net must learn to respond positively to one characteristic pattern and to reject other characteristic patterns. The neural net is trained with other characteristic patterns as examples of changed patterns. The neural net is also trained with the zero-amplitude pattern as an example of a changed pattern. The neural net becomes very sensitive to small changes in the target characteristic pattern in this manner.

Third, the pattern selected for monitoring must be sensitive to small structural changes. Several trial nets were tested for different modes, before one was deemed sensitive enough. The nets were tested for their responses to small perturbations of the cold plate.

Fourth, the neural net output must degrade gracefully in response to pattern changes. This requirement is necessary; since small non-structural changes may occur. Examples are changes in laser illumination and characteristic pattern contrast. A neural net is trained to set one of its outputs to 0.8 in response to a correct pattern and 0.2 otherwise. (These outputs are related to normalization of the neuron transfer function.) The neural net is trained to set one of its other outputs to 0.8 in response to an incorrect output and 0.2 otherwise. A neural net may learn to respond this way to 4 modes and 200 or 300 different speckle sample functions with a rms error of 0.01 or less, for example.

A neural net, meeting these requirements, was used as follows for real-time inspections of the cold plate. First, a red-line threshold was set for interpreting the same pattern output. A same pattern declaration required that the output exceed a threshold. Ideally, a threshold is set with a statistically correct calibration procedure. In the absence of a statistically correct calibration procedure, we were forced to rely on judgement and some previous experience with fan blades. The threshold was set at 0.7 or about 10 times the rms training error for whole plate inspections and 0.65 for zoomed inspections. The actual change in the output of the neural net in the zoomed case turned out to be much smaller; hence a much tighter threshold could have been used. A second requirement is a minimum difference between outputs of 0.2. The assertion of that requirement has never proved necessary.

The output of the neural network was encoded at 30 frames per second by coloring the characteristic pattern. Green represented same pattern and yellow represented changed pattern.

The neural-net-modified test procedure is then summarized as follows:

(1) Identify the normal modes of vibration of the cold plate using electronic holography.

(2) Set the amplitudes of the normal modes and record them for future reference.

(3) Select a normal mode to be inspected for changes, and select other normal modes as sample variations.

(4) Train the artificial neural network and link it with the visualization software.

(5) Excite the vibration mode of interest, and record neural-net processed stills of the mode.

(6) Commence pressurization and relaxation cycles, while monitoring the characteristic pattern with neural-net visualization.

(7) Record stills or movies of the neural-net processed characteristic patterns

during the pressurization and relaxation cycles.

(8) Record stills of the neural-net processed characteristic patterns at the end of a sequence of pressurization and relaxation cycles.

(9) Repeat steps (1) – (2) and (5) - (8) for as many sequences of pressurization and relaxation cycles as desired.

(10) Record a test set of uncorrelated speckle sample functions of the mode for quantitative evaluation by the neural network at the end of the pressurization tests.

(11) Record the real-time fringe pattern as the cold plate is gradually pressurized in order to check the quality and uniformity of construction and compare the interference patterns with the C-scans.

The results of these tests are presented in the next section.

RESULTS

The results can be summarized succinctly. Real-time holography confirms the presence of non-uniformity in the construction of the cold plate. But visual and neural-net inspections of the time-average and real-time patterns evidenced no permanent changes resulting from 3000 pressurization and relaxation cycles of the cooling passages. The neural nets detected that the mode shapes differed between the pressurized and relaxed cold plate.

The pressurization and relaxation test was interrupted every 400 cycles for the whole plate and every 250 cycles for the zoomed region to record the vibration modes and to perform a neural-net inspection. But only the results before and after the complete tests are presented; since there were no significant changes.

Figure 6 shows five characteristic patterns before execution of the pressurization and relaxation cycles. Figure 7 shows the same characteristic patterns after 2000 cycles.

Figure 8 shows five characteristic patterns of the zoomed region considered to be most suspicious by the requesters of the test. Figure 9 shows the same five characteristic patterns after 1000 pressurization and relaxation cycles. Through-holes can be seen in these figures.

For the whole-plate inspections, the neural net was trained to flag changes in the pattern shown at 1957 Hz in Fig. 6. The pattern at zero amplitude shown in Fig. 4 in large pixel format and the patterns at 2230 Hz and 2308 Hz in Fig. 6 were used as examples of other modes. That is, the neural net was trained to respond exactly the same to these modes, and the visualization software was programmed to color the characteristic patterns of these modes yellow. The visualization software was programmed to color the characteristic pattern at 1957 Hz green, if the threshold condition was met. 67 X 20 large pixels cover the whole-plate for the neural networks as in Fig. 4. Each pattern is

represented by 134 uncorrelated speckle patterns for training. A feedforward neural network with 6 hidden-layer nodes was trained. The region inspected covers 528 X 158 small pixels.

For the zoomed inspections of the region between 4 holes, a neural net was trained to flag changes in the mode at 2310 Hz. The pattern at zero amplitude shown in Fig. 5 in large pixel format and the patterns at 780 Hz and 1597 Hz in Fig. 8 were used as examples of other modes. The zoomed region is covered by 40 X 54 large pixels for the neural network as in Fig. 5. Each pattern is represented by 216 uncorrelated speckle patterns for training. A feedforward neural network with 6 hidden-layer nodes was trained. The region inspected covers 314 X 423 small pixels.

Figure 10 shows frames of the large-pixel output of the neural-net visualization software for relaxed and pressurized states of the whole cold plate. These frames were extracted from a movie recorded of several cycles.

Figure 11 shows relaxed and pressurized states for the zoomed region.

Figure 12 shows the fringe patterns from real-time holograms recorded at several values of pressure, and Fig. 13 shows a comparison between the ultrasonic C-scan and double-exposure holography.

Figure 14 shows fringe patterns from double-exposure holograms recorded after 2 cycles and 3000 cycles.

The responses of the neural nets to the relaxed plate are not perfect. Tables I and II tabulate the numbers of unchanged pattern responses after various numbers of pressurization cycles for the whole-plate and zoomed-region tests, respectively. Each number is from 20 still inspections recorded about one second apart.

For a final result, a test set of 216 uncorrelated speckle patterns of the mode at 2310 Hz was fed into the original neural network trained for the zoomed-region test. The net responded with a rms error of 0.0157; whereas the original training error was 0.0078. A response about 10 times larger than the rms error would have been necessary for the net to have flagged a significant change.

DISCUSSION OF RESULTS

The results are believed to show no significant changes after 2000 and 3000 pressurization and relaxation cycles. But the optical patterns certainly are not completely free of change. There are contrast changes between Figs. 6 and 7, in particular for the mode at 1957 Hz. That mode was selected for inspection by the neural network.

The feedforward neural network is especially good at tolerating brightness and contrast changes. This skill is especially valuable, since contrast changes are caused by optical rather than structural effects. Causes include, but are not limited to, variations in the voltage and bias point of the non-linear electro-optic modulator and speckle pattern decorrelation resulting from air currents and fluctuations in the illuminating beams. The

influence of these causes varies throughout the test day. Human observers are very sensitive to contrast changes and find it tedious and annoying, if not impossible, to interpret them.

The frequencies associated with Figs. 6, 7, 8, and 9 are used only for mode labeling. The frequencies were measured with an uncalibrated meter and the excitations were energized with an uncalibrated power oscillator. The frequencies did appear to vary somewhat from test to test, from time to time, and with changes in mode amplitude. The modes may not be pure eigenmodes; there may be non-linear effects; or the purity of excitation may vary. The variations are not sufficient to cause any confusion in mode identification.

The net flagged the mode for the pressurized state as being different from the mode for the relaxed state in Figs. 10 and 11. This result is not surprising and should not be interpreted as meaning that a change in structural integrity occurs at pressurization. Neural nets were discovered to be sensitive to mode-shape changes caused by small changes in bolt torque.

The results from real-time holography in Fig. 12 and double-exposure holography in Fig. 13 show a rather non-uniform response to pressurization. But Fig. 14, recorded from double-exposure holograms, did not show changes after 3000 pressurization and relaxation cycles.

Table I shows an anomaly at 1600 cycles, where only 10 characteristic patterns out of 20 of the relaxed plate were classified by the neural net as unchanged. This result was correlated with a period of instability of the electronic holography setup. The setup stabilized, and the number of unchanged identifications returned to a more normal value of 17 at the 2000 cycle point. The neural net is reasonably insensitive to contrast variations as discussed above, but very large changes will cause the response of the net to drop below the threshold of 0.7.

CONCLUDING REMARKS

The neural-net, holography combination has performed well for inspection of the International Space Station cold plate for structural non-uniformity and for pressure-cycle induced damage. Artificial neural-networks add objectivity, repeatability and tolerance- of-irrelevancies to a process that was previously tedious and depended on individual judgements.

The neural-net inspection process is uncalibrated at this stage. Full objectivity requires that the neural networks be trained with reliable computational models or be calibrated in a statistically acceptable manner. Hopefully, there is now enough evidence of the practical potential of neural-net inspections of characteristic patterns to justify development of the calibration procedures.

REFERENCES

1. Decker, A. J., Fite, E. B., Mehmed, O. and Thorp, S. A.: "Processing speckle patterns with model trained neural networks," *Optical Technology in Fluid, Thermal, and Combustion Flow III, Proceedings of SPIE,* **vol. 3127,** pp. 285-293, July 1997.

2. Decker, A. J., Fite, E. B., Mehmed, O. and Thorp, S. A.: "Vibrational Analysis of Engine Components Using Neural-Net Processing and Electronic Holography," *Advanced Non-Intrusive Instrumentation for Propulsion Engines, AGARD-CP-598,* pp. 33-1--33-6, May 1998.

3. Decker, A. J., Fite, E. B., Thorp, S. A. and Mehmed, O.: "Comparison of computational-model and experimental-example trained neural networks for processing speckled fringe patterns," *International Conference on Optical Technology and Image Processing Fluid, Thermal, and Combustion Flow, Proceedings of VSJ-SPIE '98,* **on compact disc in pdf, paper AB002**, December 1998.

4. Decker, A. J.: "Neural-Net Processing of Characteristic Patterns," *Topics on Nondestructive Evaluation, Volume 4, Automation, Miniature Robotics and Sensors for Nondestructive Testing and Evaluation,* Yoseph Bar-Cohen, Technical Editor, Pub. The American Society for Nondestructive Testing, Inc., Chapter 7.3, to be published.

5. EH22 Memorandum for Record 1998-55, "Metallographic Evaluation of Space Station Cold Plate SN # 47-D0044" (EH22 w/o 1998-280).

   EH22 Memorandum for Record 1998-56, "Failure Mode Analysis of Space Station Cold Plates" (EH22 w/o 1998-280).

6. Vest, C. M.: *Holographic Interferometry*. John Wiley & Sons, New York, 1979.

7. Decker, A. J.: "Holographic Cinematography of Time-Varying Reflecting and Time-Varying Phases Objects using a Nd:YAG Laser," *Optics Letters,* **vol. 7**, pp. 122-123, 1982.

8. Decker, A. J.: "Beam Modulation Methods in Quantitative and Flow Visualization Holographic Interferometry," *Advanced Instrumentation for Aero Engine Components, AGARD-CP-399*, pp. 34-1----34-16, May 1986.

9. Decker, A. J.: "Holographic interferometry with an injection seeded Nd:YAG laser and two reference beams," *Applied Optics,* **vol. 29**, pp. 2696-2700, June 1990.

10. Decker, A. J. and Izen, S. H.: "Three-dimensional computed tomography from interferometric measurements within a narrow cone of views," *Applied Optics,* **vol. 31**, pp. 7696-7706, December 1992.

11. Stetson, K. A. and Brohinsky, W. R.: "Fringe-shifting technique for numerical analysis of time-average holograms of vibrating objects," *Journal of the Optical Society of America,* **A5.** pp. 1472-1476, 1988.

TABLES

TABLE I.—NUMBER OF UNCHANGED RESPONSES IN 20 NEURAL-NET INTERROGATIONS OF RELAXED WHOLE COLD PLATE

#CYCLES	#RESPONSES
34	20
400	20
800	19
1,200	17
1,600	10
2,000	17

TABLE II.—NUMBER OF UNCHANGED RESPONSES IN 20 NEURAL-NET INTERROGATIONS OF ZOOMED REGION OF RELAXED COLD PLATE

#CYCLES	#RESPONSES
0	20
250	20
500	20
750	20
1,000	20

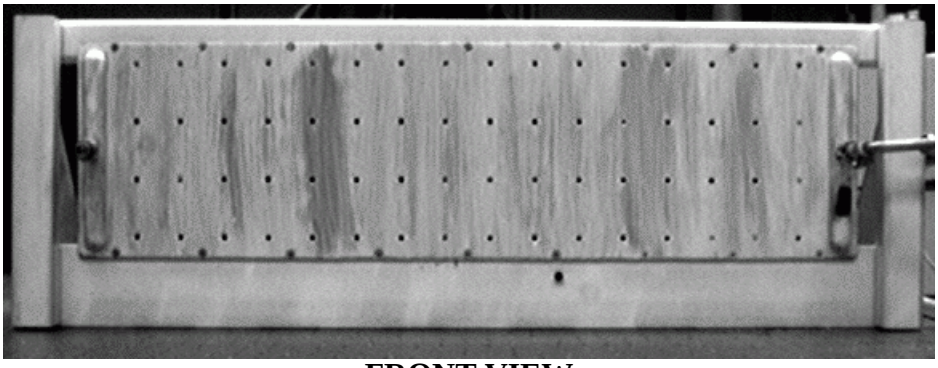

FRONT VIEW

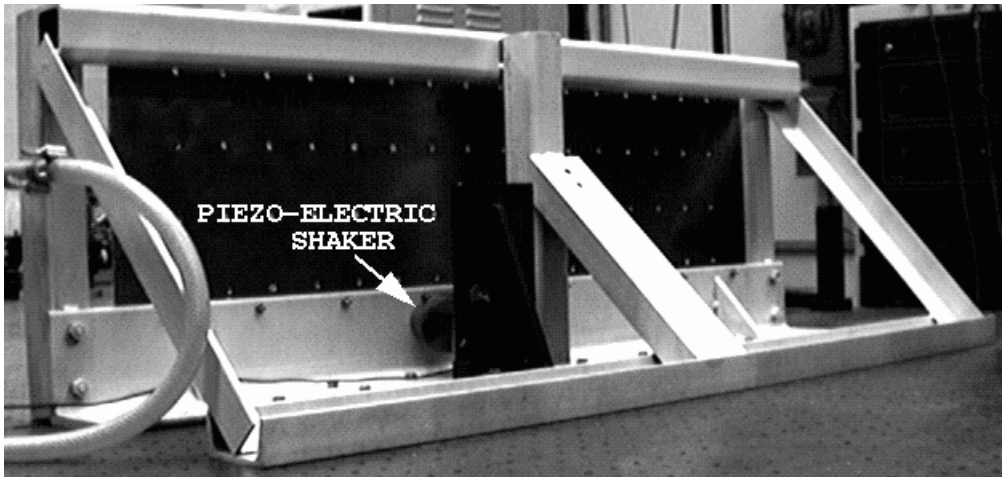

REAR VIEW

Figure 1.—Views of frame-mounted cold plate.

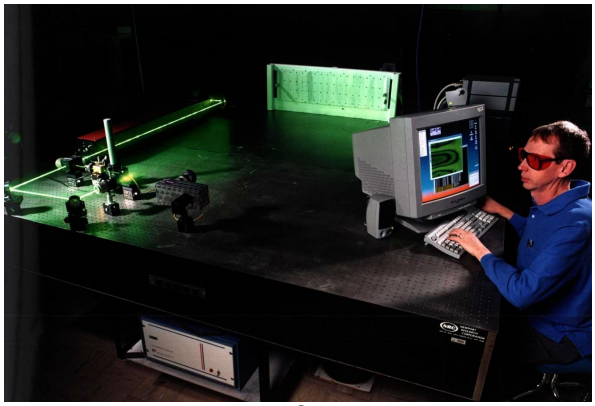

Figure 2.—Sample setup for electronic holography.

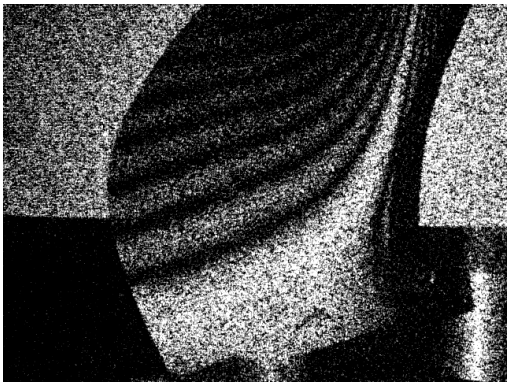

Figure 3.—Bessel fringe pattern for a vibrating blade.

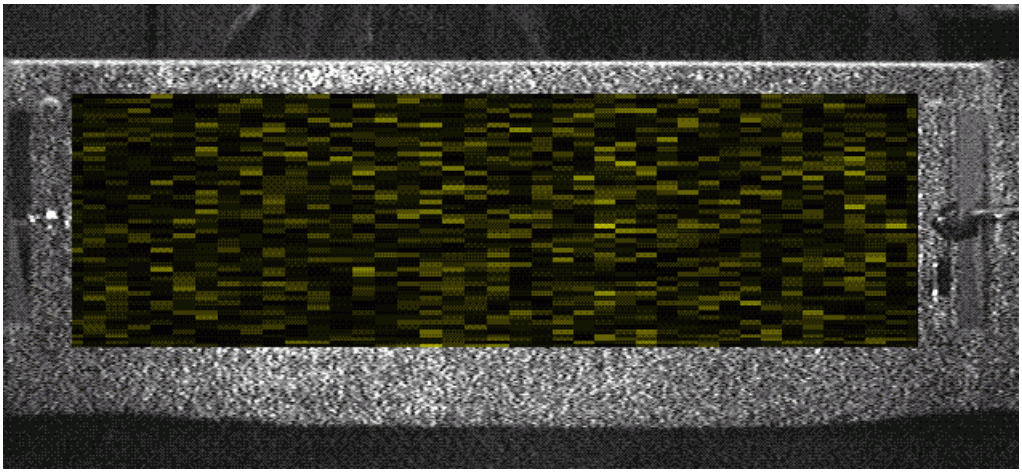

Figure 4.—Large pixel coverage for neural-net interrogation of whole plate.

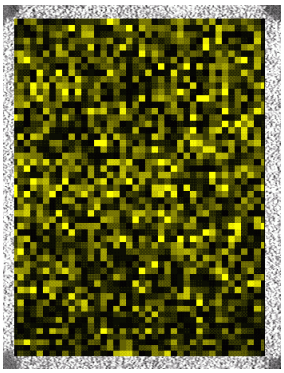

Figure 5.—Large pixel coverage for neural-net interrogation of zoomed region.

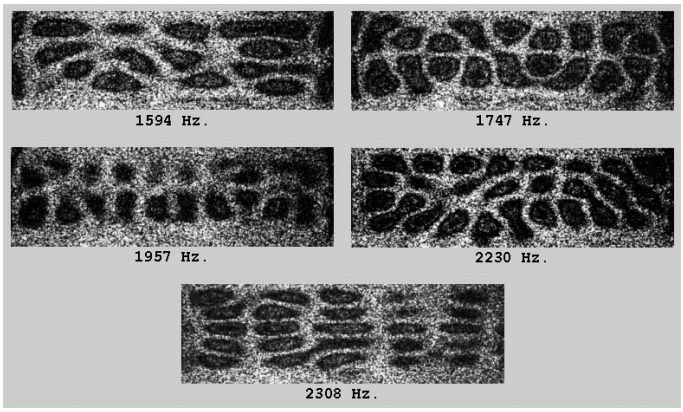

Figure 6.—Characteristic patterns before pressurization and relaxation.

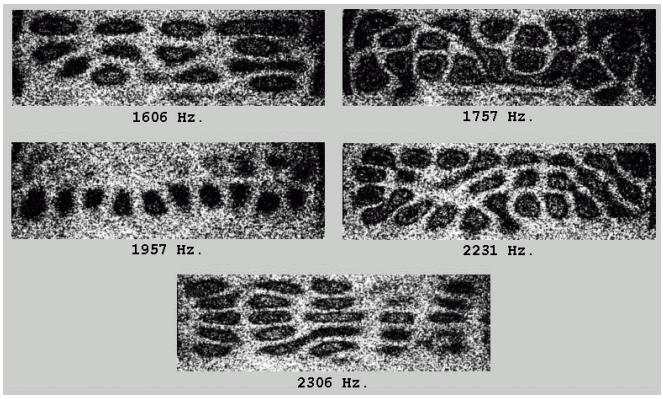

Figure 7.—Characteristic patterns after 2000 pressurization cycles.

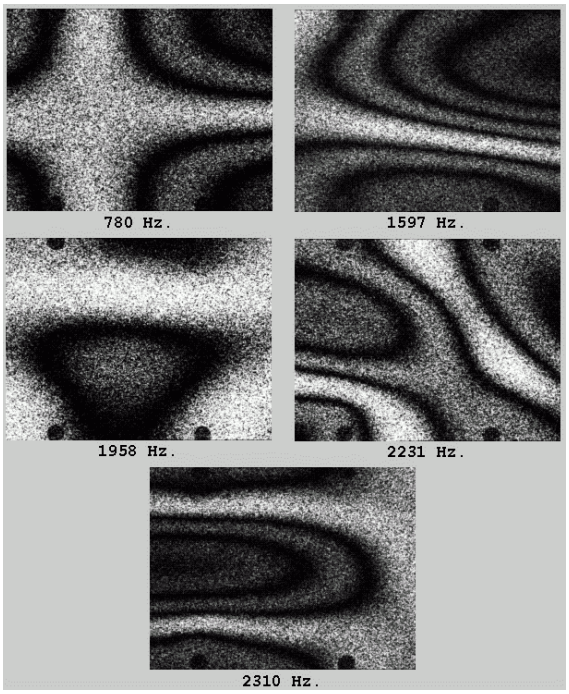

Figure 8.—Characteristic patterns for zoomed region between holes.

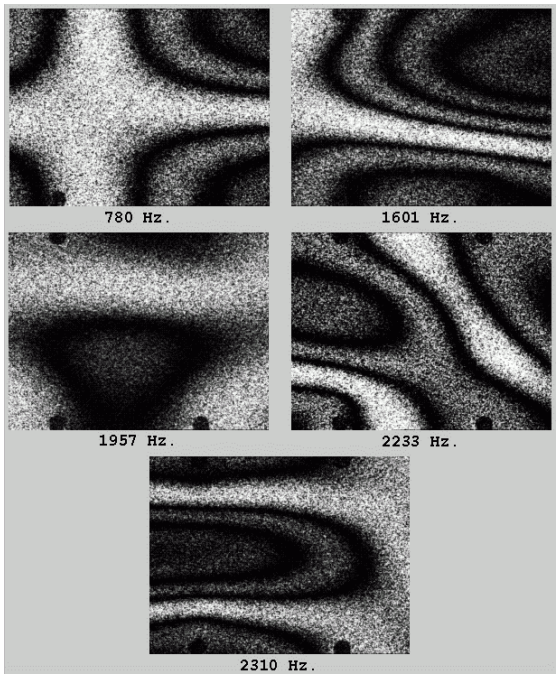

Figure 9.—Zoomed-region characteristic patterns after 1000 additional cycles.

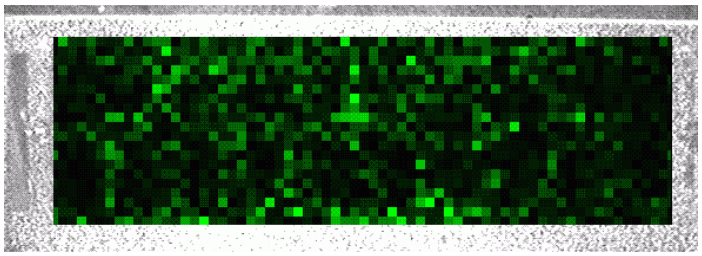

RELAXED PLATE

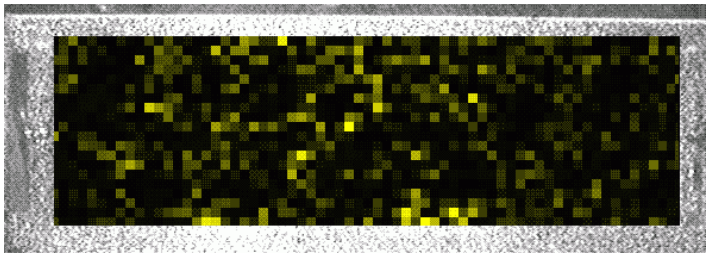

PRESSURIZED PLATE

Figure 10.—Response of neural net to relaxed and pressurized plate.

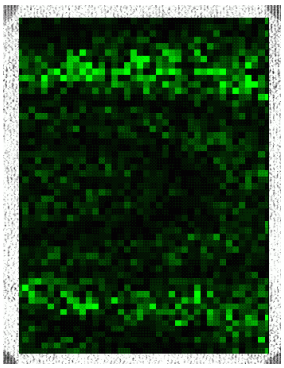

RELAXED PLATE

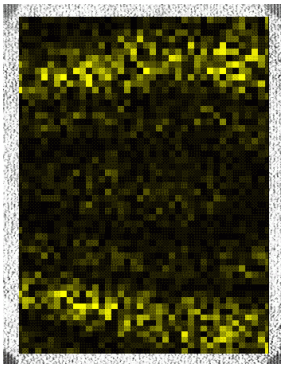

PRESSURIZED PLATE

Figure 11.—Response of neural-net in zoomed region.

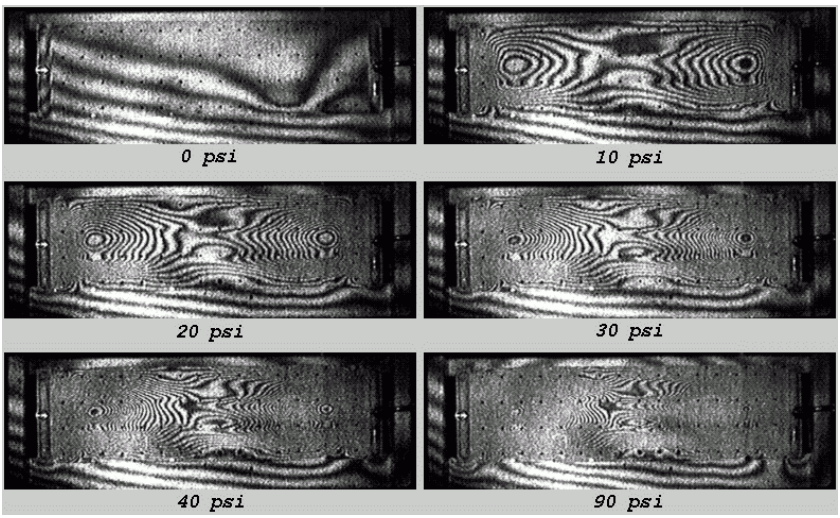

Figure 12.—Fringe patterns from real-time hologram.

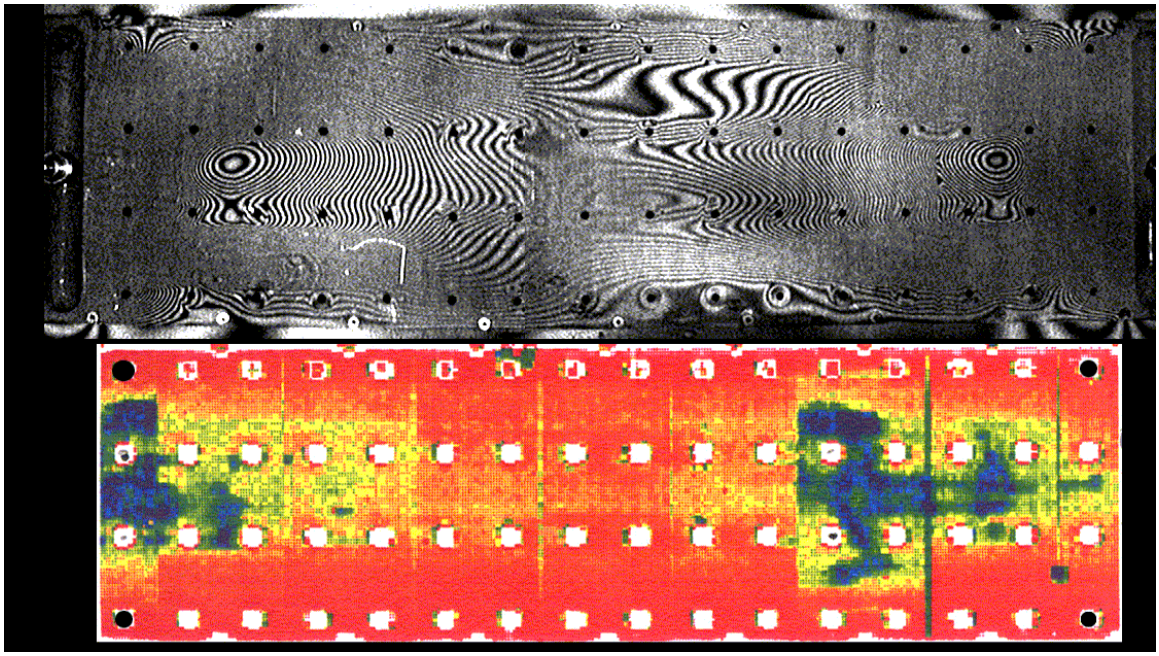

Figure 13.—Superimposed double-exposure fringe pattern and C-scan.

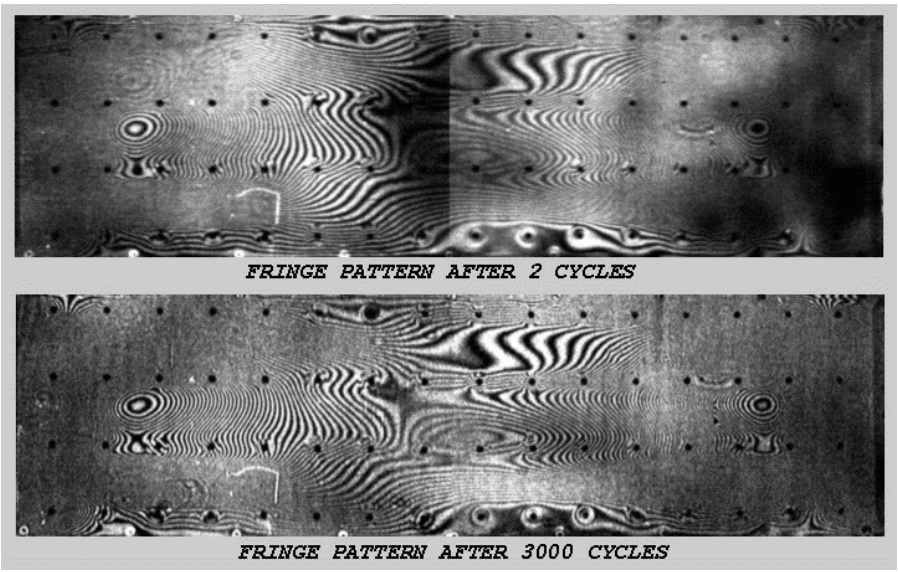

Figure 14.—Comparison of double-exposure fringe patterns at 2 and 3000 cycles.

REPORT DOCUMENTATION PAGE

Form Approved
OMB No. 0704-0188

1. AGENCY USE ONLY (*Leave blank*)	2. REPORT DATE	3. REPORT TYPE AND DATES COVERED
	August 1999	Technical Memorandum

4. TITLE AND SUBTITLE

Inspection of Space Station Cold Plate Using Visual and Automated Holographic Techniques

5. FUNDING NUMBERS

WU–478–34–10–00

6. AUTHOR(S)

Arthur J. Decker, Matthew E. Melis, and Kenneth E. Weiland

7. PERFORMING ORGANIZATION NAME(S) AND ADDRESS(ES)

National Aeronautics and Space Administration
John H. Glenn Research Center at Lewis Field
Cleveland, Ohio 44135–3191

8. PERFORMING ORGANIZATION REPORT NUMBER

E–11816

9. SPONSORING/MONITORING AGENCY NAME(S) AND ADDRESS(ES)

National Aeronautics and Space Administration
Washington, DC 20546–0001

10. SPONSORING/MONITORING AGENCY REPORT NUMBER

NASA TM—1999-209388

11. SUPPLEMENTARY NOTES

Responsible person, Arthur J. Decker, organization code 5520, (216) 433–3639.

12a. DISTRIBUTION/AVAILABILITY STATEMENT

Unclassified - Unlimited
Subject Category: 35 Distribution: Nonstandard

This publication is available from the NASA Center for AeroSpace Information, (301) 621–0390.

12b. DISTRIBUTION CODE

13. ABSTRACT ***(Maximum 200 words)***

Real-time holography has been used to confirm the presence of non-uniformity in the construction of an International Space Station cold plate. Ultrasonic C-scans have previously shown suspected areas of cooling fin disbonds. But both neural-net processed and visual holography did not evidence any progressive permanent changes resulting from 3000 pressurization and relaxation cycles of a Dash 8 cold plate. Neural-net and visual inspections were performed of characteristic patterns generated from electronic time-average holograms of the vibrating cold plate. Normal modes of vibration were excited at very low amplitudes for this purpose. The neural nets were trained to flag very small changes in the mode shapes as encoded in the characteristic patterns. Both the whole cold plate and a zoomed region were inspected. The inspections were conducted before, after, and during pressurization and relaxation cycles of the cold plate. A water-filled cold plate was pressurized to 120 psig (827 kPa) and relaxed for each cycle. Each cycle required 5 seconds. Both the artificial neural networks and the inspectors were unable to detect changes in the mode shapes of the relaxed cold plate. The cold plate was also inspected visually using real-time holography and double-exposure holography. Regions of non-uniformity correlating with the C-scans were apparent, but the interference patterns did not change after 3000 pressurization and relaxation cycles. These tests constituted the first practical application of a neural-net inspection technique developed originally with support from the Director's Discretionary Fund at the Glenn Research Center at Lewis Field.

14. SUBJECT TERMS

Space Station; Structures; Holographic interferometry; Neural nets

15. NUMBER OF PAGES

24

16. PRICE CODE

A03

17. SECURITY CLASSIFICATION OF REPORT	18. SECURITY CLASSIFICATION OF THIS PAGE	19. SECURITY CLASSIFICATION OF ABSTRACT	20. LIMITATION OF ABSTRACT
Unclassified	Unclassified	Unclassified	